# Earthshine: A Paradigm Shift for Daylight Imaging and Custody of LEO Satellites

by

Scott P. Milster (AFRL/RV), Waid Schlaegel (AFRL/RD)

Abstract

Recent daytime images of the ISS have led the authors to reevaluate the challenges of daytime imaging. Daytime images of the ISS and other satellites illuminated by Earthshine, at solar phase angles exceeding 150° are presented. These images were taken with a 2" effective aperture. The advantage of Earthshine for daytime custody is that in general, the larger the solar phase angle, the greater the Earthshine illuminating the near side of the satellite. Additionally, the presentation will discuss the strength of the Earthshine contributions, such as optimal wavebands and the spectral albedos of various terrain types, and how these need to be considered to determine the feasibility of future daytime imaging.

Acknowledgements

A special thank you to Dr. Jeannette Van Den Bosch (AFRL/RV) for her MODTRAN calculations.

# 1 INTRODUCTION

The US Air Force has been in need of the ability to observe satellites in daylight for quite some time now. Many researchers have investigated ways to meet this need. The consensus has been to observe in the infrared bands, as visible sensors tend to saturate due to the sky background (Chesser et al., 2003; Roggeman et al., 2010; Jim et al. 2010). Some researchers have tried to model the radiometry of satellites in daylight to improve predictability of observations (Cognion, 2013). The attempt by the authors was less awe-inspiring in nature. Using college interns through the Summer Scholars Program, we gave them the task to observe Low Earth Orbit (LEO) satellites in daylight. To make it achievable, we focused on the International Space Station (ISS) since it is currently the largest LEO satellite in orbit and it makes several daytime passes over the course of the summer internship. What they accomplished serendipitously led to the research contained in this paper.

# 2 METHODS, ASSUMPTIONS, AND PROCEDURES

## 2.1 Methodology

To summarize the following pages, the Sun produces an amount of irradiance (W/cm2) upon the Earth's surface. The Earth reflects a portion of this Sunlight back and has a radiance (W/cm2/ster) (aka brightness) depending upon the albedo of the Earth. This radiance produces an irradiance (W/cm2) upon a satellite orbiting above the surface of the Earth. Upon reflectance, the satellite has a radiance reflected back towards the Earth's surface. This produces an irradiance upon the Earth's surface, which we wish to intercept with a telescope. The irradiance upon the aperture of the telescope is focused upon the pixels of the telescope's camera.

The Sky also has a certain radiance (W/cm2/ster), and it depends upon the angular distance from the Sun. It too produces a certain irradiance upon the telescope. The telescope focuses this irradiance upon the camera's pixels. However, since the Sky is an extended source, it is present on multiple pixels. This includes the pixel(s) the satellite is imaged upon as well as the surrounding pixels. The object of this paper is to determine if the signal from the satellite exceeds the noise from the Sky in order to detect the contrast of the satellite over the sky.

## 2.2 Nomenclature

The authors are following the nomenclature of Smith (1990). These are summarized in Table 1. Each of these terms can be a spectral term and then each will have an additional unit of per µm. Note that $H$ and $W$ have the same units. Additionally, the authors are using the symbols in Table 2 to indicate which object has this characteristic or the last surface light is reflected from. The one assumption we make is that the Earth's land surface is Lambertian, which is a reasonable approximation. Water is not Lambertian, but it has a very low albedo ($\lesssim 0.05$) and so we will not include this in estimations of the amount of Earthshine.

*Table 1. Radiometric terminology*

| Symbol | Name | Description | Units |
|---|---|---|---|
| $P$ | Radiant power | Rate of transfer of energy | W (=J/s), or photons/s |
| $J$ | Radiant intensity | Power per unit solid angle from a source | W/ster, or photons/s/sr |
| $N$ | Radiance (aka brightness) | Power per unit solid angle per unit area from a source | W/cm$^2$/sr, or photons/s/cm$^2$/sr |
| $H$ | Irradiance | Power per unit area incident upon a surface | W/cm$^2$, or photons/s/cm$^2$ |
| $W$ | Radiant emittance | Power per unit area emitted from a surface | W/cm$^2$, or photons/s/cm$^2$ |

*Table 2. Symbols and Variables Meaning*

| Symbol/subscript | Meaning | Symbol/subscript | Meaning |
|---|---|---|---|
| $\odot$ | Sun | $\alpha$ | Albedo |
| $\oplus$ | Earth | $\theta_{\oplus}$ | Half angular size of Earth |
| $s$ | Satellite | $R$ | Radius |
| $k$ | Sky | $h$ | Altitude |
| $\ell$ | Latitude | $\lambda$ | wavelength |
| $m$ | Longitude (aka meridian) | $\phi$ | Solar zenith angle, i.e. incident angle of sunlight |
| x,y | Location on a satellite | $\beta$ | Off axis angle from satellite nadir point $\beta = 90 - a$ |
| $\omega$ | Solid angle size of source | $i$ | incident |
| $\theta'$ | Integration variable over size of source | $a$ | Altitude angle |

# 3 RESULTS AND DISCUSSION

## 3.1 Satellite Observations

### 3.1.1 ISS

The ISS was the first satellite we imaged during the daytime. One image from the pass is shown in Figure 1. This image was collected at 11:41:15 MDT on 6 July 2017, 27° from the Sun, so a solar phase angle of 153°. Its exposure was 0.10s. The telescope was a 14 inch, f/11. Celestron Schmidt Cassegrain. A photon shield upon the front of the instrument reduced the aperture to 2" and prevented light scattering off of the secondary housing. The wavelength band was 0.725-0.850µm. The range to the ISS was 726km. The pixel size was 2.3 arcseconds or 8.1m on target. The peak pixel value of the ISS is 50,000 counts, and the surrounding background is 30,000 counts.

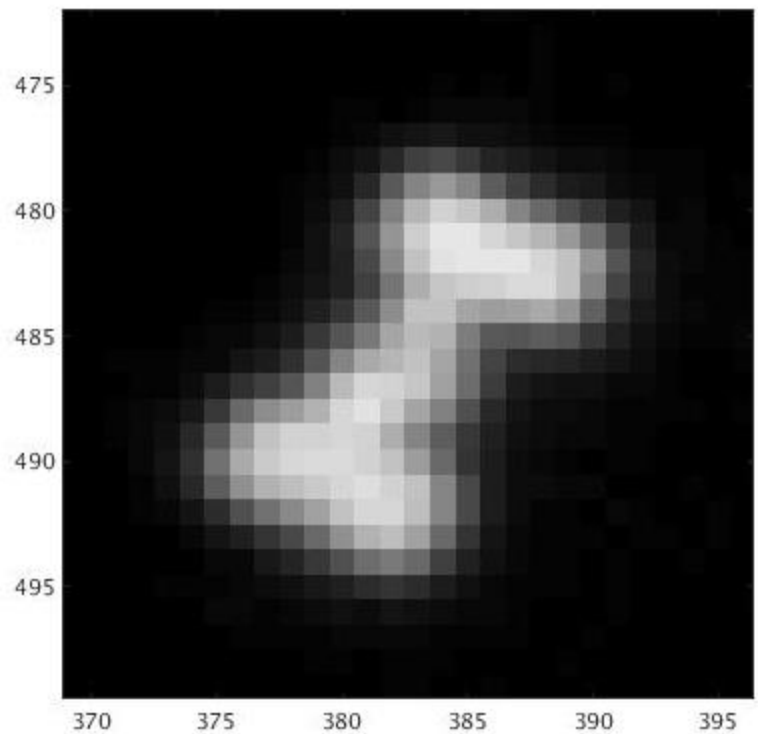


*Figure 1. ISS, 6 July 2017.*

At 27° from the Sun, this is the equivalent of the Moon being 2 days away from New Moon. The Moon is a thin crescent at this phase and the ISS is fully illuminated.

The details of the pass are shown in Figure 2, where the dashed line is the time of the image in Figure 1 was collected.

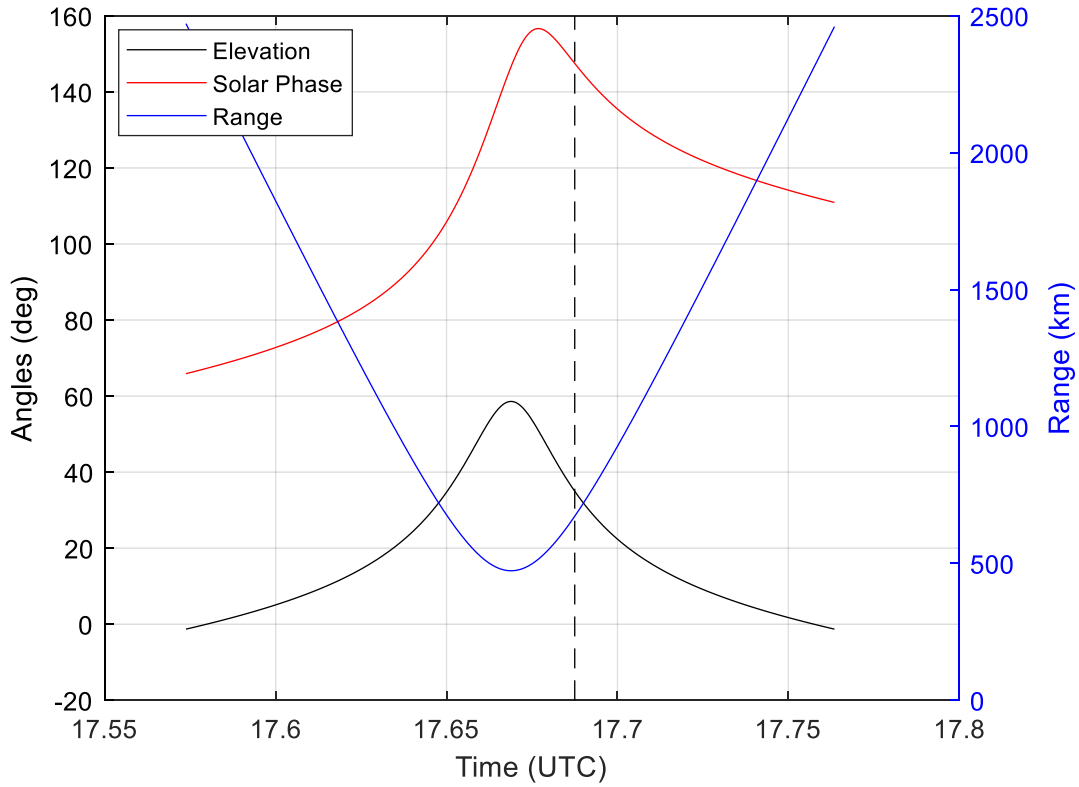


*Figure 2. ISS pass details, 6 Jul 2017.*

We improved our camera for the ISS pass we collected on 1 Jun 2018 of which one image is shown in Figure 3. This was collected at 17:15:16 MDT at an angle 9.5° from the Sun or a solar phase angel of 170.5°. The exposure was 0.09s and the band was the same. The range this time was only 590km and the pixel size is 1.8 arcseconds or 5.0m on the target.

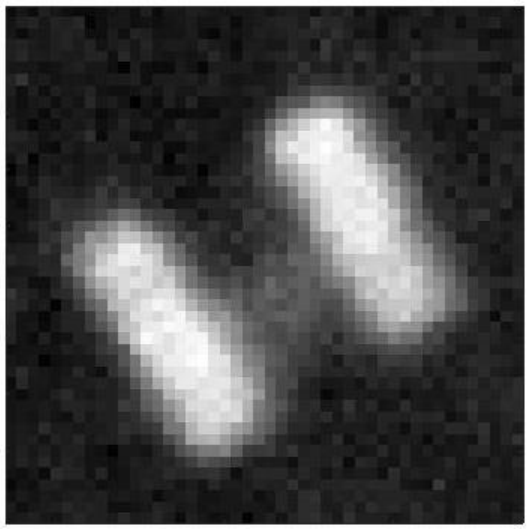

*Figure 3. ISS pass, 1 Jun 2018.*

The details of this pass are shown Figure 4 with the dashed line showing the time the image in Figure 3 was collected.

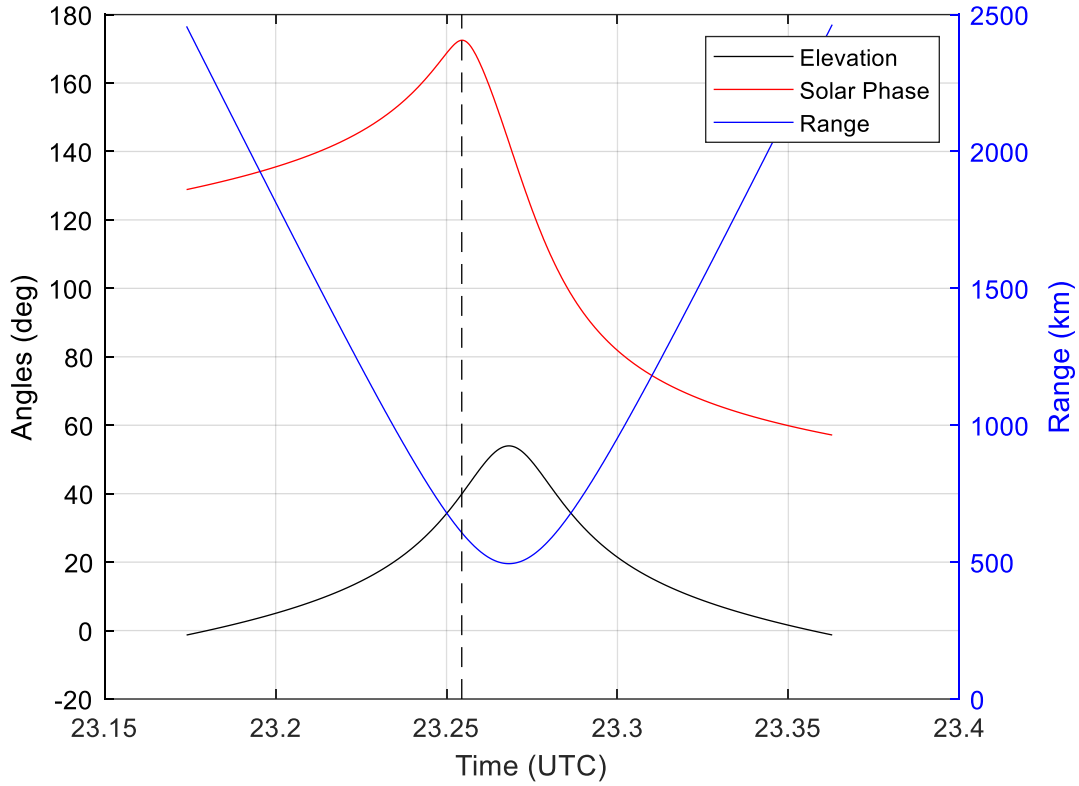


*Figure 4. Details of ISS pass of 1 Jun 2018.*

### 3.1.2 Other Satellites

Other satellites we collected daytime images of include HST and Tiangong 2. The HST pass is shown in Figure 5, with the pass details in Figure 6 where the dashed line is the time of the image shown in Figure 5. Tiangong 2 is shown in Figure 7 with the pass details in Figure 8 with the dashed showing the time the image in Figure 7 was collected.

These satellites are smaller, but are still easily found with our current instrument configuration. Figure 6

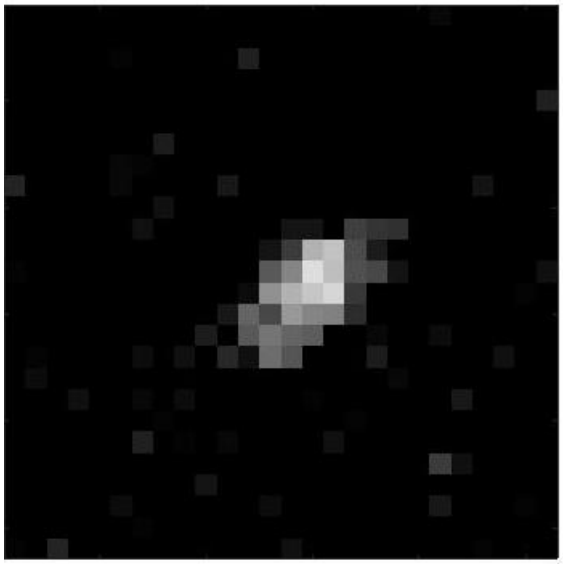

*Figure 5. HST pass on 13 Jul 2018.*

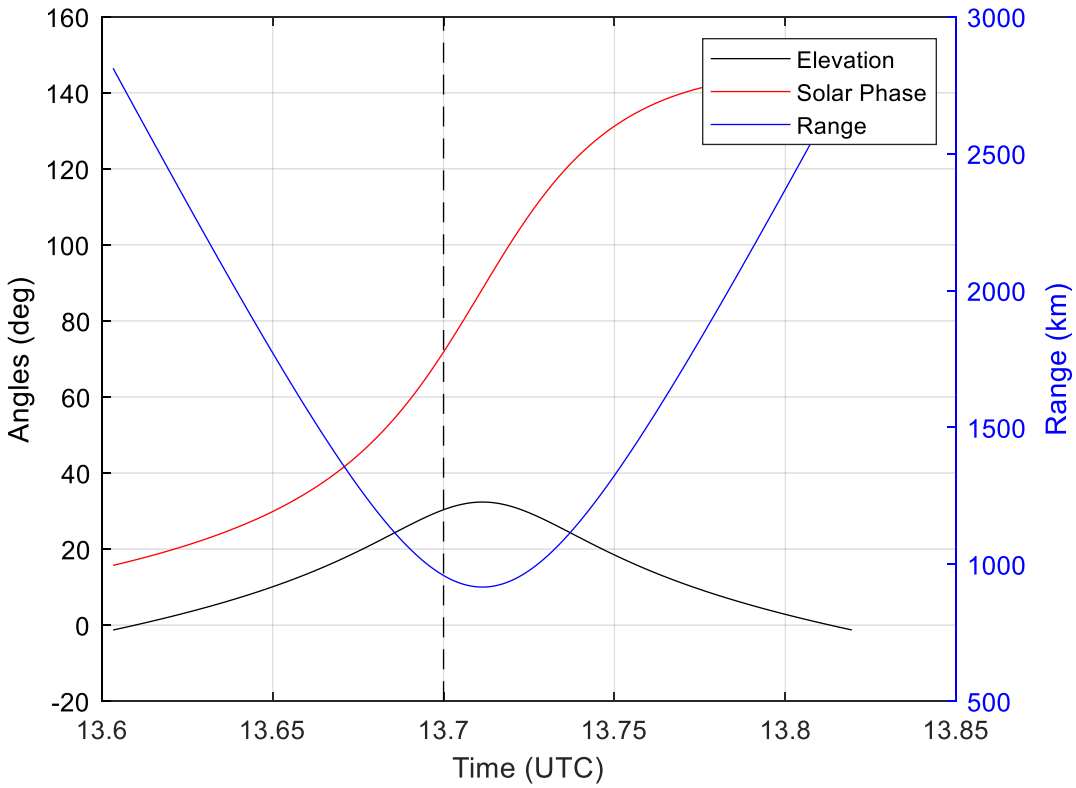


*Figure 6. Details of HST pass of 13 Jul 2018*

### 3.1.3 Tiangong 2

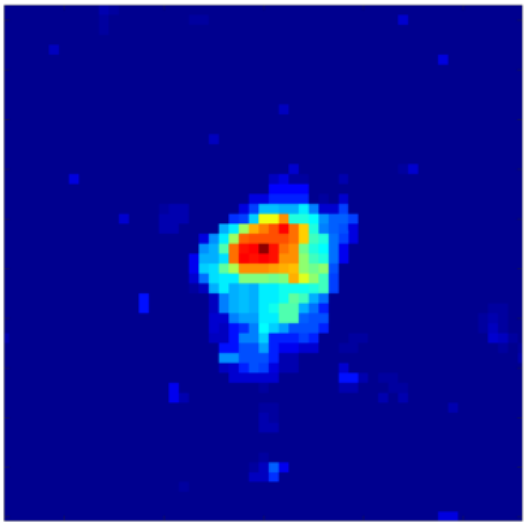

*Figure 7. Tiangon 2, pass of 22 Jun 2018.*

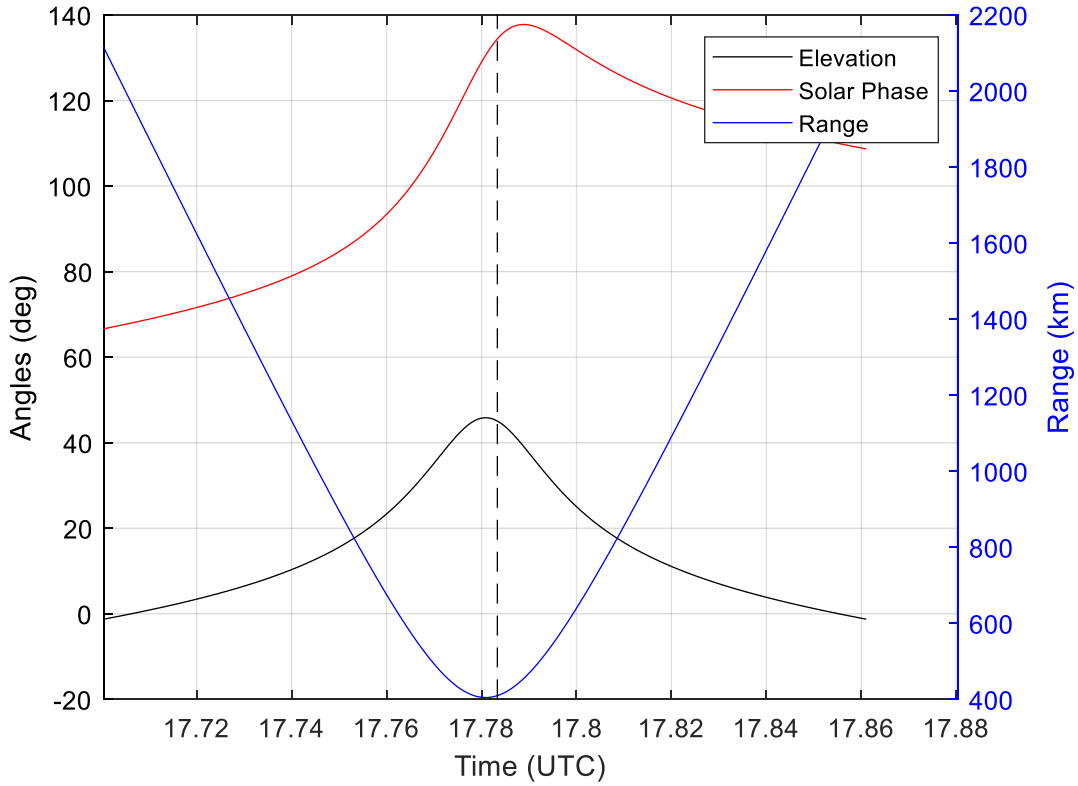


*Figure 8. Details of Tiangong 2 pass of 22 Jun 2018.*

## 3.2 Earthshine Discussion

We quickly determined that the fully illuminated images of satellites were because of Earthshine. However, the amount of Earthshine seemed quite large. To avoid as much sky background as possible, we collected images at as long a wavelength as our silcon camera and filters allowed. That led to the passband of 0.725-0.850µm. Researching the albedos of Earth materials in the Near Infrared (NIR), led us to find the albedos shown in Figure 9 (Li et al., 2017, Zhang et al., 2008). The vegetative red edge at 0.7µm is what greatly increased the amount of Earthshine that we received relative to the visible spectrum. In fact the only albedo that becomes very low in the NIR is for water. Water has an albedo of 0.01-0.05. For comparison, charcoal in the visible has an albedo of 0.05.

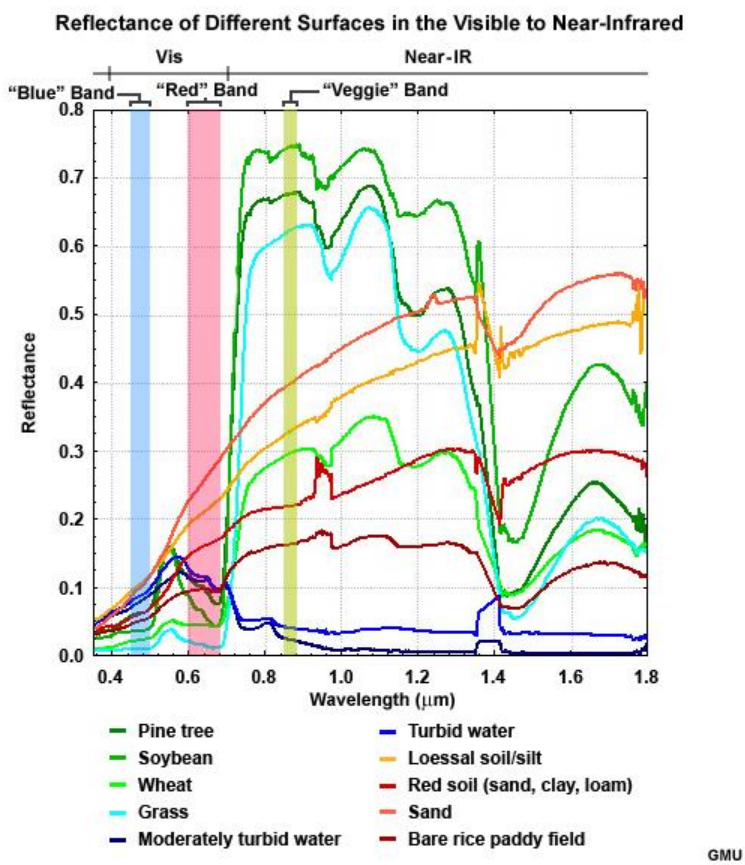


*Figure 9. Albedos of different Earth materials.*

We searched out satellite images for the NIR. The GOES-East image for the 0.86µm micron band is shown in Figure 10. The Southwestern US, part of Mexico, and the Gulf of Baha are visible. The water portion of the image is much darker than the land portion verifying what we expected from the albedos we found earlier.

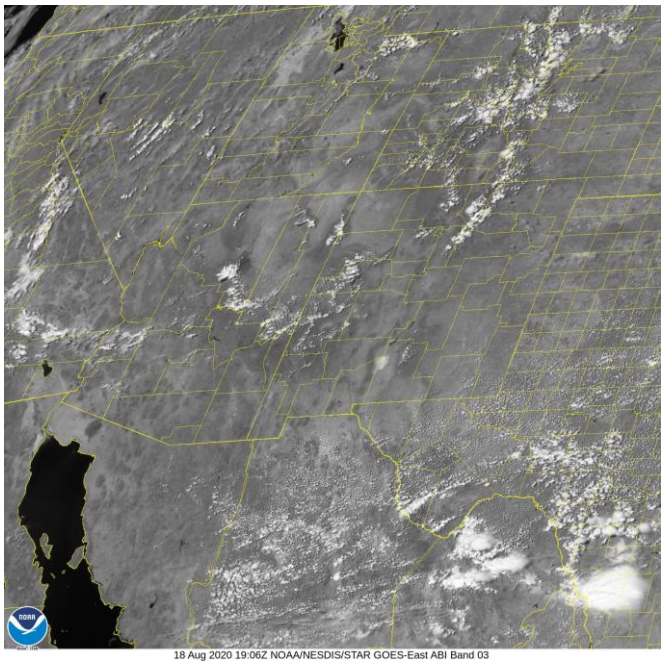


*Figure 10. NOAA, GOES-East Image of Southwest 0.86μm.*

## 3.3 Theoretical Derivations

### 3.3.1 Spectral Earthshine incident upon a Satellite

In order to compare our data collections with theory, we first must derive the equations for the satellite brightness as a function of solar irradiance and the Earth albedos. The spectral solar irradiance from MODTRAN, $H_{\odot}(\lambda)$, at the top of Earth's atmosphere is shown in Figure 11, along with the Sun's blackbody curve.

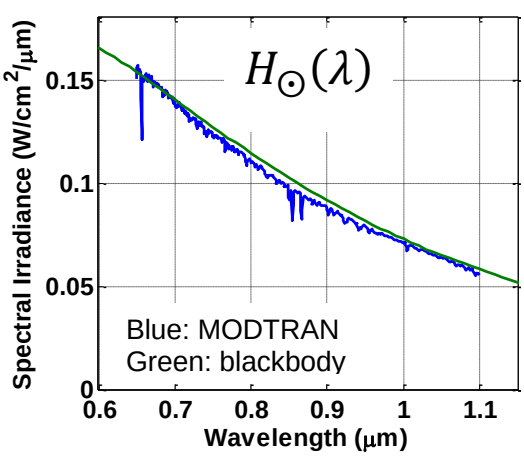


*Figure 11. Solar Irradiance at Earth's Top of Atmosphere.*

It is easy to determine from geometry the angular radius of the Earth from a satellite at altitude h, and is shown in Eq 1.

$$\theta_{\oplus} = \arcsin \frac{R_{\oplus}}{R_{\oplus} + h}. \tag{1}$$

To determine the light incident upon the Earth's surface, we need the Sun's solar zenith angle, $\phi(lat, lon)$, at every point that is visible from the satellite. At every point this is

$$H_{i\odot}(\lambda, \ell, m) = H_{\odot}(\lambda) \cos \phi(\ell, m). \tag{2}$$

Then to determine the radiant emittance of a location we need to include the local albedo and we get

$$W_{\oplus}(\lambda, \ell, m) = \alpha_{\oplus}(\ell, m, \lambda) H_{i\odot}(\lambda, \ell, m). \tag{3}$$

The relationship between spectral radiant emittance ($W$, units W/cm$^2$/µm) and spectral radiance ($N$, W/cm$^2$/sr/µm) for Lambertian surfaces is Smith's (1990) Equation 8.4 so

$$W_{\oplus}(\lambda, \ell, m) = \pi N_{\oplus}(\ell, m, \lambda). \tag{4}$$

By combining Eqs 2-4, the radiance of the Earth's surface at a particular location is given by

$$N_{\oplus}(\ell, m, \lambda) = \frac{1}{\pi} \alpha_{\oplus}(\ell, m, \lambda) \cos \phi(\ell, m)\, H_{\odot}(\lambda) \tag{5}$$

To find the irradiance from the Earth's surface incident upon a satellite (height h above the surfaces) we must integrate the radiance from the Earth's surface in sight of the satellite by using Smith's Eq 8.5:

$$\begin{aligned} H_{\oplus}(h, \lambda) &= \int_{A_{\oplus}} \frac{N_{\oplus}(\ell, m, \lambda)\ \cos^4 \theta'}{h^2} dA_{\oplus} \\ H_{\oplus}(h, \lambda) &= \frac{1}{\pi} \int_{A_{\oplus}} \frac{\alpha_{\oplus}(\ell, m, \lambda) \cos \phi(\ell, m)\, H_{\odot}(\lambda) \cos^4 \theta'}{h^2} dA_{\oplus}. \end{aligned} \tag{6}$$

Note, in deriving Eq. *6* the only assumption made is that the Earth is Lambertian. While not true for water, as noted earlier the albedo for water is extremely low, $\lesssim 0.05$ and so it will contribute very little to the amount of Earthshine incident upon a satellite. For land, assuming the Earth is Lambertian is a very good approximation.

### 3.3.2 Satellite Spectral Radiance

At this point, it is useful to use average values in order to integrate Eq 6 and determine a first estimation of the irradiance incident upon the satellite and to be able to compare with our observations. The result simplifies to:

$$H_{\oplus}(h, \lambda) = \bar{\alpha}_{\oplus}(\lambda) \cos \bar{\phi}\, H_{\odot}(\lambda) \sin^2 \theta_{\oplus}. \tag{7}$$

As the satellite is so much smaller than the Earth, except for self-shading, this is the irradiance each part of the satellite receives.

The emittance from the satellite is

$$W_s(\lambda) = \alpha_s(\lambda)\bar{\alpha}_\oplus(\lambda)\cos\bar{\phi}\, H_\odot(\lambda)\sin^2\theta_\oplus \tag{8}$$

This ignores any effects of shadowing or multiple reflection. The radiance from the satellite is

$$N_s(\lambda) = \frac{1}{\pi}\alpha_s(\lambda)\bar{\alpha}_\oplus(\lambda)\cos\bar{\phi}\, H_\odot(\lambda)\sin^2\theta_\oplus \tag{9}$$

### 3.3.3 Satellite Spectral Irradiance Incident upon a Telescope

From Smith's (1990) Eq 8.8, we find that the on-axis irradiance of a source of radiance $N$ that subtends a small solid angle $\omega$ is

$$H_{on-axis} = N\omega. \tag{10}$$

This is the irradiance directly below the satellite. The illumination off axis by an angle, $\beta$, is reduced according to Smith's Eq 8.9

$$H_\beta = H_{on-axis}\cos^4\beta. \tag{11}$$

One of the factors of $\cos\beta$ in Eq 11 is due to the illumination being spread across a surface perpendicular to the on-axis direction, which can be eliminated by a telescope pointing at the satellite. Additionally, for a satellite, $\beta$ is related to its altitude $a$ by

$$\beta = 90 - a. \tag{12}$$

Taking Eqs 9-12 we find that the irradiance from a satellite incident upon a telescope pointing at it is

$$H_s = \omega N_s\cos^3\beta = \omega N_s\sin^3 a \tag{13}$$

where $a$ is the altitude angle of the satellite from the observer, and $\omega$ is the solid angle of the satellite. Since the solid angle is small, we can write this as

$$H_s = \frac{A_s}{h^2}N_s\sin^3 a \tag{14}$$

where $A_s$ is the cross sectional area of the satellite parallel to the Earth's surface (i.e. the portion illuminated by Earthshine), and $h$ is the orbital height of the satellite. $H_\beta$ (W/cm$^2$) is the irradiance produced at the observer's location. Substituting in Eq 9 we get

$$H_s = \frac{A_s}{h^2}\sin^3 a\,\frac{1}{\pi}\alpha_s(x,y,\lambda)\bar{\alpha}_\oplus(\lambda)\cos\bar{\phi}\, H_\odot(\lambda)\sin^2\theta_\oplus \tag{15}$$

This is the irradiance incident upon the telescope.

# 4 COMPARING OBSERVATIONS WITH THEORY

To photometrically calibrate observations of satellites we have relied upon calibrated stars in the past. Unfortunately, very few stars could be seen during the daytime with our instrument. We decided the only way to calibrate would be off of the sky itself. MODTRAN is a software program to model atmospheric propagation of electromagnetic radiation from 0.2 to 100 µm. It is a data driven model that relies upon sensors located at various locations. One location is Albuquerque NM. Its outputs include the solar spectral irradiance at the top of the atmosphere and the sky spectral radiance.

Taking the MODTRAN solar spectral irradiance output (Figure 11) as an input to Eq 15, and making assumptions about the other inputs as shown in Table 3, we calculate the spectral radiance of the ISS as shown in Figure 1. The results are displayed in Figure 12. The spectral radiance, which is independent of the size of the satellite actually becomes brighter than the sky once the wavelength is greater than about 0.9µm.

*Table 3. Assumed values for calculations.*

| Quantity | Assumed Value |
|---|---|
| $\bar{\phi}$ | 23.6° |
| $\theta_{\oplus}$ | 70° |
| $\bar{\alpha}_s$ | 0.25 |
| $\bar{\alpha}_{\oplus}$ | 0.25 |
| | |

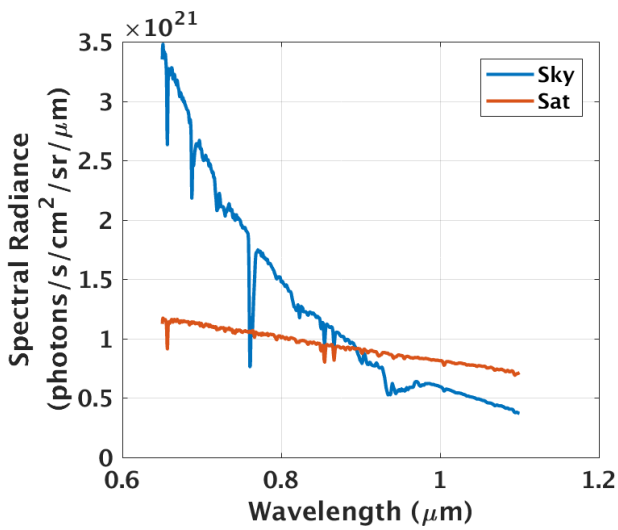


*Figure 12. Spectral Radiance of Sky and ISS from Figure 1.*

We then integrated over the bandwidth of our instrument to determine if the ratio of the sky to the satellite brightness is consistent. The theoretical calculations show that we expect 29,300 photons incident upon the telescope from the sky and 19,100 photons incident upon the telescope

from the satellite for a ratio of 0.65. From the data, the background averages to about 30,000 counts and the satellite is about 20,000 counts above that, for a ratio of 0.67. The gain of our camera was about 0.98 e/count so for the pixels where the counts were around 20,000 for the satellite, the single pixel SNR is 110 for Figure 1. Similar calculations were done for the second ISS pass. Due to the different camera and smaller pixels, the single pixel SNR for Figure 3 is about 35.

# 5 FUTURE WORK AND CONCLUSIONS

## 5.1 Future Work

We would like to be able to derive albedos or Earthshine by utilizing Landsat and/or GOES satellite images. This capability would allow the prediction of satellite brightness hours or days before a satellite pass and would be very useful in planning observations.

Improving instrument scatter reductions would also enable us to image fainter and smaller objects or objects in higher orbits even close to the Sun.

## 5.2 Conclusions

While the exact amount of Earthshine may be difficult to predict, the simple fact of the much greater amount of Earthshine over land enables satellites to be imaged in the daytime even close to the Sun. Such capabilities will be very useful, as it will enable optical methods to determine satellite orbits and greatly reduce the error ellipsoid around satellites. A much smaller error ellipsoid is needed with the launching of mega constellations.

## References


Chesser, D. E., Vunck, D., Born, T., Axelson, W., Rehder, K., & Medrano, R. S. (2003, August). NIR daylight acquisition sensor improves mission capabilities. In *Acquisition, Tracking, and Pointing XVII* (Vol. 5082, pp. 1-12). International Society for Optics and Photonics.

Cognion, R. L. (2013). Observations and modeling of GEO satellites at large phase angles. *AMOS Proceedings*.

Jim, K. T., Wolfshagen, R., Gibson, B., Pier, E., Hodapp, K., & Onaka, P. (2011, September). The HANDS-IONS Daytime Camera for GEO Satellite Characterization. In *Proceedings of the Advanced Maui Optical and Space Surveillance Technologies Conference, held in Wailea, Maui, Hawaii*.

Li, S., Sun, D., Goldberg, M. D., Sjoberg, B., Santek, D., Hoffman, J. P., ... & Holloway, E. (2018). Automatic near real-time flood detection using Suomi-NPP/VIIRS data. *Remote sensing of environment*, *204*, 672-689.

Roggemann, M. C., Douglas, D., Therkildsen, E., Archambeault, D., Maeda, R., Schultz, D., ... & Kihei, H. I. (2010). Daytime Image Measurement and Reconstruction for Space Situational Awareness Applications (Paper ID number 4231324). *amos*, E17.

Smith, W. J. (1990). Modern Optical Engineering, 2nd edition. McGraw Hill.

Zhang, Y.X., Zhang, I.J., Huang, Y.F., Rong, Z.G., Hu, X.Q., Liu, J.J., Zhang, G.S., (2008). Spectral Data Sets for Satellite Calibration Site and Typical Earth Objects. M., China Meteorological Press.